Polymer Testing 100 (2021) 107227

Contents lists available at ScienceDirect

Polymer Testing

journal homepage: www.elsevier.com/locate/polytest

# Design, manufacturing and preliminary assessment of the suitability of bioplastic bottles for wine packaging

C. Aversa [a], M. Barletta [a,*], A. Gisario [b], E. Pizzi [a], R. Prati [c], S. Vesco [d]

[a] Dipartimento di Ingegneria, Università degli Studi Roma Tre, Via Vito Volterra 62, 00146, Roma, Italy
[b] Dipartimento di Ingegneria Meccanica e Aerospaziale, Sapienza Università degli Studi di Roma, Via Eudossiana 18, 00184, Roma, Italy
[c] Caviro SCA, Via Convertite 8, 48018, Faenza, RA, Italy
[d] Dipartimento di Ingegneria dell'Impresa, Università degli Studi di Roma Tor Vergata, Via del Politecnico 1, 00133, Roma, Italy

ARTICLE INFO

*Keywords:*
*Bioplastic*
*Extrusion blow molding*
*Wine bottle*
*Material processing*
*Characterization*

ABSTRACT

The aim of this study is to evaluate the suitability of bioplastic bottles for wine packaging. The wine is largely packaged in glass bottles, although alternative solutions such as laminate, plastic and bag-in-box packaging are decidedly widespread on the market by virtue of their ease of use and low cost, especially for the so-called entry-level products. However, packaging involving the partial or exclusive use of plastic is the subject of discussion in the scientific community, by virtue of the persistence of plastic materials in the environment at the end of the product life cycle. A solution that could reconcile the practicality and low cost of plastic packaging with a reduced environmental footprint is the replacement of fossil-based plastics with compostable bioplastics. The latter biodegrade if properly treated at the end of their life, limiting the environmental footprint of the packaging. Bioplastics are, however, more complex to process than conventional plastics, also presenting a higher cost. The objective of this study is therefore the manufacture of prototype bottles in bioplastic for the packaging of wine by means of an extrusion blow molding process, as well as the evaluation of the main thermo-mechanical and physical properties of the same.

## 1. Introduction

The packaging of food products is increasingly the subject of heated debate in the scientific community [1]. Sophisticated packaging solutions make it possible to isolate and protect the food of the surrounding environment, ensuring food safety and significantly extending the shelf life of the product [2,3]. In this way, the packaging becomes the tool to reduce food waste, helping to reduce the massive environmental impact generated by the latter. On the other hand, the useful life of the packaging is extremely short, so they must be properly treated at the end of their lives. In particular, plastic packaging requires particular care as it is often complex to recycle and when disposed of in landfills, it has very long persistence times in the environment (even over a century) [4]. The packaging of wine and, more generally, alcoholic beverages falls within the scope of the previous problems. It is strictly necessary to pack the wine properly, in order to allow it to be stored and, in some cases, to refine over time. However, the management of the end of life of bottles for wine packaging is an absolute priority of the community [5]. The wine is normally packaged in glass, which guarantees the almost total isolation of the product from the external environment (in particular, from the air and light radiation), ensuring its correct conservation over time. In general, glass bottles are recyclable, but they are heavy, fragile and impractical [6]. In the lower segments of the market, alternative packaging solutions have been imposed such as plastic bottles (in particular, in polyethylene terephthalate (PET)), laminated cardboard packaging and bag-in-box [7,8]. These packaging solutions combine low cost with lightness and unbreakability, therefore with ease of use. The end-of-life management of non-glass packaging for wine is, however, very complex. PET bottles are recyclable, but, in the case of wine, they must be carefully washed before they can be recycled, which complicates the process. The PET bottles for water that do not need to be washed are sent for recycling for 50% and only 10% is reused for the production of new bottles [9]. These numbers would be dramatically reduced when a pre-wash was required in the recovery cycle. Laminated cardboard and bag-in-box packaging pose an even greater problem as they consist of multi-materials, the separation of which is expensive and complex, making the recycling operation economically unsustainable [10,11]. In this context, compostable bioplastic bottles could be a valid

* Corresponding author.
*E-mail address:* massimiliano.barletta@uniroma3.it (M. Barletta).

https://doi.org/10.1016/j.polymertesting.2021.107227
Received 17 February 2021; Received in revised form 2 May 2021; Accepted 9 May 2021
Available online 15 May 2021
0142-9418/© 2021 The Authors. Published by Elsevier Ltd. This is an open access article under the CC BY-NC-ND license (http://creativecommons.org/licenses/by-nc-nd/4.0/).

**Table 1**
Description of the formulations (note that the nomenclature of the formulations starts from ES4 as formulations ES1, ES2 and ES3 were not investigated further because they were not processable in extrusion blow molding).

| | EStr. | ES4 | ES5 | ES6 | ES7 |
|---|---|---|---|---|---|
| **Components** | **wt%** | **wt%** | **wt%** | **wt%** | **wt%** |
| **PLA Luminy LX175** | 76,64 | 0,00 | 0,00 | 0,00 | 0,00 |
| **PLA Luminy L105** | 0,00 | 8,00 | 10,00 | 12,00 | 12,00 |
| **PLA Luminy L175** | 0,00 | 56,00 | 50,00 | 42,00 | 36,00 |
| **PBS FZ91 (E)** | 0,00 | 16,50 | 15,50 | 14,50 | 12,50 |
| **PBS FD 92 (PBSA)** | 19,16 | 0,00 | 0,00 | 0,00 | 0,00 |
| **PLA Luminy D120** | 0,00 | 2,00 | 2,00 | 2,00 | 2,00 |
| **TALC IMERYS LUZENAC HAR W92** | 0,00 | 13,45 | 18,45 | 25,50 | 30,50 |
| **OTHER ADDITIVES** | 4,20 | 4,05 | 4,05 | 4,00 | 7,00 |

alternative for wine packaging [12]. They have lightness and unbreakability, therefore practicality of use. In addition, they are compostable, so end of life management is extremely simple. They can be directly delivered to the green fraction, without the need for any washing to be composted. The compost obtained can be used as fertilizer in the vine growing process, closing a virtuous cycle [13]. Bioplastics are more expensive than fossil-based plastics (up to about three times). They are more complex to transform in the bottle manufacturing process [14]. Furthermore, the thermo-mechanical, chemical and physical performances of bioplastics could be unsatisfactory, especially for wine packaging. In fact, wine requires a series of measures to avoid alteration of the product, such as minimizing the gas permeability of the bottle and reducing the transmission of light radiation [15].

The objective of this study is therefore the manufacture of prototype bottles in bioplastic, in particular, in PLA/PBS blends, for the packaging of wine. In addition, attention is paid to the evaluation of the thermo-mechanical and physical properties of the bottle, in order to assess its suitability for wine packaging. The experimental results have shown that the correct design of the bioplastic material allows the prototyping of high-quality bottles, which have proved to be suitable for packaging wine. Therefore, bioplastic bottles, although still burdened by the excessive cost of the raw material, are undoubtedly a solution of significant interest for packaging with a low ecological footprint of wine and, more generally, of alcoholic beverages.

## 2. Experimental

### 2.1. Materials

Five types of bioplastic materials have been studied. To prepare the PLA/PBSA blend, PLA Luminy LX175 was chosen. It is a high viscosity, fully biobased PLA homopolymer suitable for injection molding, supplied by Total Corbion PLA DV, Gorinchem, Netherlands. It features 96% L-isomer polylactic acid (PLA), slow to crystalize [16]. It has a density of 1.24 g/cm$^3$, a melting peak temperature of about 155 °C, a glass transition temperature of about 60 °C, an elastic modulus of 3500 MPa and a tensile strength of 50 MPa according to ISO 527–1. Luminy LX175 grade is characterized by a melt flow index (MFI) of 3 g/10 min according to ISO 1133-A at 190 °C, 2.16 kg. It has a molecular weight of 1.63 × 10$^5$ kDa and a polydispersion index of less than 2. PBS FD92 is a bio-based polybutylene succinate-co-adipate (PBSA) produced from polymerization of bio-based succinic and adipic acid and 1,4-butanediol, supplied by PTT MCC Biochem Company Limited (Bangkok, Thailand). It has a melting peak temperature of about 84 °C, a glass transition temperature of ~ -45 °C, a density of 1.24 g/cm$^3$, an MFI according TO ISO 1133 of 4 g/10 min at 190 °C, 2.16 kg. It has a tensile strength of 27–32 MPa and an elongation at break of about 580–600% according to ISO 527–2. The other polymeric blends are based on 99% L-isomer PLA as the main polymeric phase. Polybutylene succinate (PBS) is, instead, used as secondary polymeric phase. PLA Luminy L105 is a high heat, low viscosity biobased PLA homopolymer suitable for injection molding, supplied by Total Corbion PLA DV, Gorinchem, Netherlands. PLA Luminy L175 is a high heat, high viscosity biobased PLA homopolymer suitable for extrusion, supplied by Total Corbion PLA DV (Gorinchem, Netherlands). Both grades have a density of 1.24 g/cm$^3$, an L-isomer content of 99%, a melting peak temperature of about 175 °C, a glass transition temperature of about 60 °C, an elastic modulus of 3500 MPa and a tensile strength of 50 MPa according to ISO 527–1. Luminy L105 grade has a melt flow index (MFI) of 30 g/10 min according to ISO 1133-A at 190 °C, 2.16 kg. It has a molecular weight of approximately 7.9 × 10$^4$ kDa and a polydispersion index lower than 2. Luminy L175 grade has a melt flow index (MFI) of 3 g/10 min according to ISO 1133-A at 190 °C, 2.16 kg. It has a molecular weight of 1.63 × 10$^5$ kDa and a polydispersion index of less than 2. BioPBS FZ91 is a bio-based PBS produced from polymerization of bio-based succinic acid and 1,4-butanediol, supplied by PTT MCC Biochem Company Limited (Bangkok, Thailand). It has a melting peak temperature of about 118 °C, a glass transition temperature of ~ -32 °C, a density of 1.26 g/cm$^3$, an MFI according to ISO 1133 of 4 g/10 min at 190 °C, 2.16 kg. It has a tensile strength of 30 MPa and an elongation at break of about 170% according to ISO 527–2. PLA Luminy D120 is, instead, a biobased PLA with a D-isomer content of 99% and a melt flow index (MFI) of 10 g/10 min according to ISO 1133-A at 190 °C, 2.16 kg. Luminy D120, when combined with PLA homopolymers, acts as nucleating agent. Talc Luzenac HAR W92 was supplied by Imerys S.A. (Paris, France). It is micronized talc with an average size of the granulometric distribution varying between 2 and 10 μm. This talc is micro-lamellar, particularly useful as a reinforcing element in bioplastic compounds and as a nucleating agent [17]. Rheological additives (specifically, a melt strength enhancer (<1%), an impact modifier (<1%), a chain extender (~0.1%)) and lubricants (internal (<1%) and mold release (<1%), with the overall amount reported in Table 1) are used to improve the behavior of the materials during the compounding process and, subsequently, to improve the behavior of the compounds during the extrusion blow molding of the bottles. Formulations EStr, ES4, ES5 and ES6 feature the same type of additives with minimum difference (0.2%) that are ascribable to the different proportions used with respect to the polymeric matrix. In the formulation ES7, the same additives of the formulation ES6 are used (4.00%), but an additional 3% of impact modifiers was included to increase the flexibility of the blend that involve the higher amount of talc (i.e., the overall amount of impact modifiers was therefore kept lower than 4 wt %).

Table 1 summarizes the five formulations investigated. The ratio of PBSA in PLA in the formulation Estr is 1:4. The ratio of PBS to PLA (i.e., the sum of L105, L175 and D120) is always 1:4 in all the other formulations.

### 2.2. Processing

After drying for 5.5 h at 55 °C (Drymax E60, Wittmann Bottenfeld, Wien, Austria), the formulations were compounded by a corotating twin screw extruder with a screw diameter of 27 mm (ZSE 27 MAXX, Leistritz Extrusionstechnik GmbH, Nuremberg, Germany) equipped with two gravimetric feeders (Flexwall Plus Feeder FW 40/5, Brabender Technologie GMBH & Co, Duisburg, Germany) and a side-feeder (LSB 26, Leistritz Extrusionstechnik GmbH, Duisburg, Germany) to dose powder additives and one volumetric feeder (EC30 M, BHT Srl, Camposanto (MO), Italy) to dose pellets. The barrel of the extruder is divided into 10 controlled temperature sections. The volumetric metering feeder with paddle-massaged flexible hopper for pellets (Flexwall Plus Feeder, Brabender Technologie GMBH & Co, Duisburg, Germany) is located in zone (barrel) 1. The gravimetric small-size twin screw metering feeder for packing powders (Laboratory Loss-In-Weight Feeders, Brabender Technologie GMBH & Co, Duisburg, Germany) is located in zone (barrel) 4. Lastly, the twin-screw extruder is equipped with a vent position in zone (barrel) 6 and a liquid ring vacuum pump in zone (barrel) 9. Filtering section is in zone (barrel) 10, immediately before the die head of the twin-screw extruder apparatus. The twin-screw corotating extruder is

**Table 2**
Setting of the twin-screw extruder processing parameters.

| | | EStr. | ES4 | ES5 | ES6 | ES7 |
|---|---|---|---|---|---|---|
| **Temperature, zone 1** | °C | 160 | 170 | 170 | 170 | 175 |
| **Temperature, zone 2** | °C | 175 | 180 | 180 | 180 | 185 |
| **Temperature, zone 3** | °C | 175 | 180 | 180 | 180 | 182 |
| **Temperature, zone 4** | °C | 168 | 175 | 175 | 175 | 175 |
| **Temperature, zone 5** | °C | 162 | 170 | 170 | 170 | 170 |
| **Temperature, zone 6** | °C | 160 | 168 | 168 | 168 | 168 |
| **Temperature, zone 7** | °C | 155 | 165 | 165 | 165 | 165 |
| **Temperature, zone 8** | °C | 152 | 162 | 162 | 162 | 165 |
| **Temperature, zone 9** | °C | 150 | 160 | 160 | 160 | 165 |
| **Temperature, die head** | °C | 175 | 185 | 185 | 185 | 190 |
| **Screw speed** | rpm | 500 | 550 | 550 | 600 | 600 |
| **Volumetric feeding** | | 34% | 31% | 30% | 24% | 19% |
| **Gravimetric feeding** | kg/h | – | 7.95 | 10.86 | 12.63 | 14.82 |

also equipped with the following auxiliary apparatus: (1) a temperature controlled strand die head flange mounted to the last barrel of the extruder with 3 bores 2 mm in diameter for the manufacturing of the plastic strands; (2) a cooling bath fitted with several strand guide rolls to guide the strands in the water for cooling purposes (necessary to simplify the cutting process of the pellet at the end of the compounding extrusion process); (3) a strand blowing unit for strand pre-drying; and (4) a speed-controlled strand pelletizer (Haake Fisions PP1 pelletizer POSTEX, Thermo Fisher Scientific, Waltham, MA, USA) with frequency converter and range adjustment of pellets length for pellet cutting. Table 2 summarizes the setting of the processing parameters of the twin-screw extruder. The rotation speed of the screws was set at 500–600 rpm. The rotation speed of the side feeder screws was kept constant at 256 rpm. The volumetric feeding was decreased at any time the amount of mineral in the formulation was increased. The mass flow of the extruder was about 40 kg/h. The pressure of the polymer melt varied in a range between 35 and 50 bar, with an absorption of about 40% (with respect to the maximum).

The equipment for extrusion blow molding is constituted by a 60 mm single screw, L/D = 30 (ratio of the length of barrel L to the diameter of the screw D), temperature-controlled extruder (EBM 60/30, Serioplast Spa, Urgiano (BG), Italy) with a metered feeding hopper. The extruder was equipped with three different zones with independent temperature control: feeding zone; conveying zone, extrusion zone. The die head is equipped with an annular die, 20 mm in diameter, for the parison manufacturing (i.e., parison formation stage). The equipment operates in semi-continuous mode, with the parison extruded and cut off by a heated knife (surface temperature of the knife is set at 300 °C and the clearance between mold and knife is set at 0.1 mm). The blown zone is equipped with a calibrated mandrel that is inserted in the parison during the blowing process to form the neck of the bottle and two cooled metal semi-molds, where the parison is pinched (i.e. pinch off stage) and air is, then, blown into the parison, inflating it into the shape of the hollow bottle (i.e., blow-up stage). After cooling down, the bottle is finally ejected from the mold and stored for further evaluations.

### 2.3. Characterization

Thermal analysis of the compounds and bottles after processing was performed by Differential Scanning Calorimetry (DSC) (DSC 3 Star System, Mettler Toledo, Columbus, Ohio, USA). Approximately 7–10 mg of material were placed in a hermetic aluminum pan under 25 ml/min nitrogen flow. The samples were submitted to a heating scan from 20 °C to 270 °C at a heating rate of 10 °C/min. The weight crystallinity degree (Xc, %) of PLA was calculated according to Eq. (1):

$$X_c(\%) = \frac{\Delta H_m - \Delta H_{cc}}{\Delta H_m^0 \cdot \varphi} \cdot 100 \quad (1)$$

where $\Delta H_m$ and $\Delta H_{cc}$ (J/g) are the experimental melt enthalpy and cold crystallization enthalpy, respectively. The experimental melt enthalpy is calculated as the area under the melting peak and the experimental cold crystallization enthalpy is the area of the cold-crystallization peak, which appear in the thermogram. The theoretical melt enthalpy of PLA is $\Delta H^0_m$ is 93.1 J/g [18]. Φ is the actual weight fraction of polymer in the formulation. In particular, for the formulations containing PDLA, equations used to evaluate the total crystallinity of PLA also consider, the crystalline aliquot 1:1 od the stereo-complex phase. In agreement with [19], in this case, the overall ponderal degree of crystallinity of the PLA ($X_c$, %) is given by the sum of the crystallinity of the PLA phase PLA ($X_{c,PLLA}$) and of the stereo-complex phase ($X_{c,sc}$):

$$X_{c,PLLA}\ (\%) = \frac{\Delta H_{m,\ PLLA} - \Delta H_{cc}}{\left(\Delta H^0_{m,PLA} * (\phi_{PLLA} + \phi_{PDLA})\right)} * 100$$

$$X_{c,sc}\ (\%) = \frac{\Delta H_{m,\ sc}}{\left(\Delta H^0_{m,sc} * (\phi_{PLLA} + \phi_{PDLA})\right)} * 100$$

$$X_c\ (\%) = X_{c,sc} + X_{c,PLLA}$$

$\Delta H^0_{m,sc}$ is the theoretical value of the melting enthalpy of the PLA stereo-complex. A reference enthalpy value of 142 J/g in agreement with [20] was set. In this case, given the low % of the PDLA phase in the formulations, the calculation of the crystallinity term relating to the stereo-complex was neglected. Furthermore, the calculation was applied only to the first scan thermogram, which is directly connected to the properties of the product as obtained downstream of the process. However, for additional analyses, three scans were performed on the bottles: the first heating was followed by a cooling from 270 °C at room temperature to 10 °C/min and, finally, a second heating from 20 to 270 °C always at 10 °C/min. The impact resistance of the bottles was studied through drop tests from a 90 cm high worktop. The bottles were individually filled with 187.5 ml of water and sealed with flexible film to prevent liquid spillage. The drop test was carried out by placing the single bottle, thus filled and sealed, in a vertical position on a work surface 90 cm from the ground. The bottle was delicately positioned in an unstable equilibrium condition along the edge of the top and dropped following minimal input. At this point, appropriate photographic documentation was collected certifying the break or not at the point of impact, on a statistic of three samples for each formulation of the series. If the bottle did not break, a second test was carried out on it, starting from a reclined position on one side (i.e., horizontal) to simulate a different overturning condition when falling. The tests were replicated, at least, five time to ensure reproducibility and repeatability of the experimental findings. The visual evaluation of the damages on the body of the bottles allowed to discriminate the test response of the different materials under study. Light transmission spectra of the bottles were tested by UV-VIS spectrophotometry (V670, Jasco, Easton, MD, USA). The optical system includes a Rowland off-circle arrangement, a single monochromator, with double beam type. The spectral bandwidth is 1 nm. The range of wavelength investigated was from 190 to 1000 nm, with a scan speed of 1000 nm/min, a slew speed of 24,000 nm/min and a step of 0.5 nm. Oxygen permeability was tested with a three sensors measurement apparatus suitable for $O_2$, $H_20$ e $CO_2$ sequential analysis (TotalPerm, PermTech Srl, Pieve Fosciana (LU), Italy) according to the ASTM D3985 regulation. The analysis of the bottles was led in the following conditions: $O_2$: 23 °C, 15% RH; $H_2O$: 23 °C, 85% RH. Carrier flow was set at 11.78 ml/min, in high conditioning mode. End of the measurement was set in automatic mode (stability 0.5%). The last test involved the tasting of the wine packaged in the various bottles by a panel of three expert tasters, in order to identify changes in the characteristics of the product depending on the material used to manufacture the bottle. Tests were replicated three times.

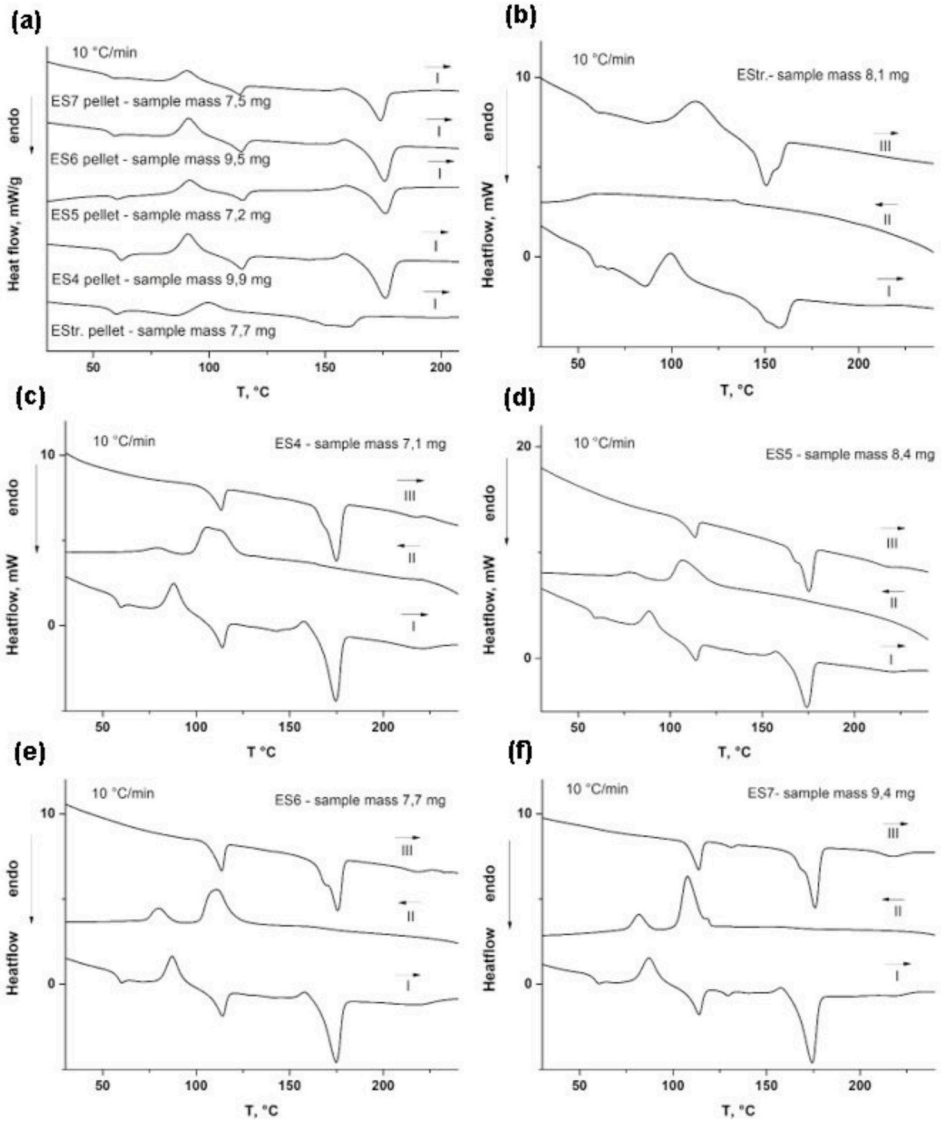


**Fig. 1.** Thermograms of the different formulations investigated: (a) compounds; (b) EStr bottle; (c) ES4 bottle; (d) ES5 bottle; ϵ ES6 bottle; (f) ES7 bottle.

**Table 3**
Thermal transitions of the different formulations investigated.

| | Scan | $(T_g)_{PLA}$, °C | $(T_{cc})_{PLA}$, °C | $(T_{hc})_{PLA}$, °C | $(T_m)_{PLA}$, °C | $(T_m)_{PLA,sc}$, °C | $(T_m)_{PBSA}$, °C | $(T_m)_{PBS}$, °C |
|---|---|---|---|---|---|---|---|---|
| EStr. | I | 57.86 | 99.44 | – | 158.62 | \ | 84.88 | \ |
| ES4 | I | 59.80 | 90.83 | 158.37 | 175.76 | 221.86 | \ | 113.98 |
| ES5 | I | 58.00 | 91.59 | 159.08 | 176.08 | 222.54 | \ | 114.66 |
| ES6 | I | 56.38 | 91.13 | 158.49 | 175.40 | 221.05 | | 113.62 |
| ES7 | I | 56.40 | 90.43 | 157.65 | 173.61 | 222.69 | \ | 112.98 |

**Table 4**
Thermal transitions evaluated on the bottles fabricated with the different materials.

| | Scan | $(T_g)_{PLA}$, °C | $(T_{cc})_{PLA}$, °C | $(T_{hc})_{PLA}$, °C | $(T_m)_{PLA}$, °C | $(T_m)_{PLA,sc}$, °C | $(T_m)_{PBSA}$, °C | $(T_m)_{PBS}$, °C |
|---|---|---|---|---|---|---|---|---|
| EStr. | I | 56.76 | 99.37 | – | 157.16 | \ | 85.53 | \ |
| ES4 | I | 56.91 | 87.95 | 157,33 | 174.11 | 221.65 | \ | 113.79 |
| ES5 | I | 57.63 | 88.69 | 157.15 | 173.56 | 222.06 | \ | 113.67 |
| ES6 | I | 57.58 | 87.12 | 157.85 | 174.48 | 220.84 | | 113.98 |
| ES7 | I | 58.23 | 86.96 | 157.54 | 173.99 | 221.25 | \ | 113.66 |

## 3. Results and discussion

Fig. 1 shows the thermograms of the compounds and bottles fabricated with the different formulations. Table 3, Table 4, Table 5 and Table 6 summarize the main results. Downward peaks are associated with energy absorptions (endothermic peaks). The EStr compound has a

**Table 5**
Heats absorbed or released during the DSC scans of the different formulations under investigation (first scan).

| | $(\Delta Hm)_{PBSA}$, J/g | $(\Delta Hm)_{PBS}$, J/g | $(\Delta Hm)_{PLLA}$, J/g | $(\Delta Hcc)_{PLA}$, J/g | $(\Delta Hhc)_{PLA}$, J/g | %, $X_{cPLA}$ |
|---|---|---|---|---|---|---|
| EStr. | 2.59 | \ | 22.63 | 14.14 | – | |
| normalized | 13.52 | \ | 29.53 | 18.45 | – | 11.9 |
| ES4 | \ | 6.49 | 24.59 | 15.90 | 4.24 | |
| normalized | \ | 39.33 | 38.42 | 24.84 | 6.63 | 7.5 |
| ES5 | \ | 6.78 | 19.12 | 9.23 | 4.62 | |
| normalized | \ | 43.74 | 31.87 | 15.38 | 7.7 | 9.6 |
| ES6 | | 6.50 | 22.25 | 14.04 | 3.54 | |
| normalized | \ | 44.83 | 41.20 | 26.0 | 6.56 | 9.3 |
| ES7 | \ | 6.89 | 19.40 | 10.05 | 2.40 | |
| normalized | \ | 55.12 | 40.42 | 20.94 | 5.0 | 15.6 |

**Table 6**
Heats absorbed or released during the DSC scans of the different bottles under investigation (first scan).

| | $(\Delta Hm)_{PBSA}$, J/g | $(\Delta Hm)_{PBS}$, J/g | $(\Delta Hm)_{PLLA}$, J/g | $(\Delta Hcc)_{PLA}$, J/g | $(\Delta Hhc)_{PLA}$, J/g | %, $X_{cPLA}$ |
|---|---|---|---|---|---|---|
| EStr. | 2.0 | \ | 22.32 | 20.0 | – | |
| normalized | 10.44 | \ | 29.12 | 26.10 | – | *3.2* |
| ES4 | \ | 8.79 | 24.26 | 12.34 | 4.98 | |
| normalized | \ | 53.27 | 37.91 | 19.28 | 7.78 | *11.7* |
| ES5 | \ | 8.26 | 22.96 | 11.58 | 3.83 | |
| normalized | \ | 53.29 | 38.27 | 19.3 | 6.38 | *13.5* |
| ES6 | \ | 8.15 | 21.58 | 10.09 | 2.22 | |
| normalized | \ | 56.21 | 39.96 | 18.69 | 4.11 | *18.5* |
| ES7 | \ | 6.63 | 19.89 | 9.66 | 1.77 | |
| normalized | \ | 53.04 | 41.44 | 20.13 | 3.69 | *19.0* |


**Fig. 2.** Image of the compounds achieved by tween-screw extrusion (grades EStr., ES4, ES5, ES6, ES7).

**Table 7**
MFI (g/10 min) calculated at 230 °C under a load of 2,16 kg.

| Formulation | *MFI (Trial 1)* | *MFI (Trial 2)* | *MFI (Trial 3)* | *Density, g/cm³* |
|---|---|---|---|---|
| ***EStr*** | 57.0 | 60.9 | 59.0 | 1.02 |
| ***ES4*** | 32.0 | 32.7 | 32.4 | 1.12 |
| ***ES5*** | 25.0 | 26.1 | 28.3 | 1.15 |
| ***ES6*** | 26.94 | 27.1 | 27.2 | 1.18 |
| ***ES7*** | 20.3 | 19.2 | 19.4 | 1.20 |

**Table 8**
Processing parameters during extrusion blow molding of the different bottles.

| Formulation | *Feeding Zone, T (°C)* | *Conveying Zone, T (°C)* | *Extrusion Zone, T (°C)* | *Die-Head, T (°C)* |
|---|---|---|---|---|
| ***EStr*** | 135–155 | 165–175 | 165–175 | 170 |
| ***ES4*** | 150–170 | 180–190 | 180–190 | 185 |
| ***ES5*** | 150–170 | 180–190 | 180–190 | 185 |
| ***ES6*** | 150–170 | 180–190 | 190–200 | 190 |
| ***ES7*** | 150–170 | 180–190 | 190–200 | 190 |

glass transition temperature at ~58 °C ascribable to the PLA. It has a wide melting band, with a peak at about 85 °C which can be attributed to PBSA. It has a cold crystallization peak, ascribable to PLA, at ~100 °C. At ~159 °C, a further wide band ascribable to the melting of PLA can be noticed. This peak is weak as the PLA with 96% of isomer – L is slow to crystallize. The compounds ES4, ES5, ES6 and ES7 have glass transition temperatures in the range of 56–60 °C. The formulations that contain higher talc concentration have, surprisingly, the lowest glass transition temperatures of ~56 °C. The talc can probably interpose between the PLA molecules in the amorphous phase, leading to the reduction of physical interactions among the polymeric chains and, consequently, cause the reduction in the glass transition temperature. This result matches the analysis of the thermograms in Ref. [21]. In this work, the glass transition of PLA/PBS blends (4: 1) is studied as the talc content varies from 0 to 20% by weight. Indeed, the formulation ES7 was the only one to involve impact modifiers, that can be a role in determining the $T_g$. The impact modifiers chosen are based on methyl methacrylate -butadiene-styrene (MBS) whose glass transition is far below zero (~−80 °C)). Impact modifiers were often found to affect glass transition, by decreasing it as they interpose between polymeric chains (Wu, Bosnyak e Sehanobish 1998), (Lasciano et al., 2019). In particular, Petchwattana et al. demonstrated that limited addition of acrylates inside PLA matrix (as low as 1%) can affect the glass transition temperature of PLA, decreasing it of 2–3 °C (Petchwattana et al., 2017). The $T_g$ is not visible for blends containing 20% talc, while it is visible for the non-talc-containing blends. In addition, as the concentration of talc increases, the corresponding $T_g$ is lower.

All the compounds that contain talc exhibit a neat cold

**Fig. 3.** Parison after right setting of the process parameters of the extrusion blow molding.

crystallization peak at about 91 °C. This peak occurs at over 8 °C lower than the corresponding peak observed on the EStr formulation in accordance with (W. P.-A. Pivsa-Art 22–24 April 2013). The talc is therefore an active nucleant for the crystallization of PLA. The concentration of talc does not appear to influence the cold crystallization peak observed for the ES4, ES5, ES6 and ES7 compounds, as it is introduced in the formulation in far excess. The different proportions of PLA extrusion grade (Luminy L175/LX175) and injection (Luminy 105) grade also do not appear to affect the temperature of cold crystallization. However, the PLA grades used in the ES4, ES5, ES6 and ES7 compounds are made of 99% L-isomers, unlike what happens for the EStr formulation. The increase in L isomer content accelerate the crystallization rate of PLA and, consequently, the cold crystallization temperature is expected to decrease. Therefore, the simultaneous presence of talc with PLA grades with a high content of isomer - L justifies the reduction in the cold crystallization temperature observed on ES4, ES5, ES6 and ES7 compounds.

The ES4, ES5, ES6 and ES7 formulations also show hot crystallization at temperatures of ~158–159 °C. The melting temperature is found between 174 and 176 °C, about 16/18 °C more than the corresponding melting temperature shown by the EStr blend, which, however, contains PLA with a lower content of isomer - L. The melting temperature of PBS is also visible in the ES4, ES5, ES6 and ES7 compounds at temperatures of ~113–114 °C. The crystallinity content and, consequently, the normalized heat of fusion of the ES4, ES5, ES6 and ES7 compounds increases as the talc content increases both for the PLA (degree of crystallinity which increases from 7.5% for the ES4 formulation to 15.6% for the ES7 formulation) and for the PBS aliquots. The talc, therefore, determines an effective nucleating action on both PLA and PBS polymeric phases inside the compounds. It should be emphasized that the Estr formulation, while presenting an apparently slower crystallization kinetics, nevertheless obtains a good degree of crystallinity (11.9%). In the absence of talc, it is likely that both the secondary PBSA phase dispersed within the main phase in PLA [22] and the stearamide used in formulation (EBS) [23,24] both act as nucleating agents for the PLA/PBSA blend. Yet, the extrusion compound of the EStr is the more troublesome, seen the scarce melt strength of the PBSA. The compounding process slows down, allowing more time to the material to crystallize, differently from what happens for the PLA/PBS compounds.

The analysis of the thermograms on the bottles add further information. Fig. 1b–f shows the thermograms of the first, second and third scans performed on the bottles fabricated with the different formulations, specifically EStr, ES4, ES5, ES6 and ES7. The results are strictly correlated to the type of formulations used in the manufacturing of the bottle. In particular, the thermograms of the EStr bottle shows in the first heating scan the glass transition of the PLA (Fig. 1b) at temperature slightly lower than 60 °C, the broad and shallow endothermic band of the PBSA melting at around 85 °C, the exothermic peak of cold crystallization of the PLA at about 99 °C and, lastly, the endothermic heat of fusion of the PLA itself (peak at ~157 °C). This last peak shows a slight shoulder peak at slightly lower temperature, which is attributable to the α′ crystals of PLA [25]. The second scan is almost a flat line, where, however, it is still possible to clearly distinguish the glass transition of the PLA. The third scan shows the same peaks of the first scan, which are however shifted at different temperatures. The bottles in EStr are characterized by a crystallinity of just 3.2%, rather lower than the crystallinity measured on the Estr compound. Bottle cooling in the mold is very quick, not allowing the formation of significant amount of PLA crystals, as it happens during the extrusion compounding of the EStr blend. Nucleation of EStr is therefore very slow, as it does not involve


**Fig. 4.** Bottles fabricated by extrusion blow molding of the formulations EStr, ES4, ES5, ES6 and ES7.

**Table 9**
Control plan of the bottles fabricated with the different formulations.

| Test | UOM | EStr | ES4 | ES5 | ES6 | ES7 |
|---|---|---|---|---|---|---|
| Weight | g | 24.7 ± 0.88 | 23.06 ± 0.28 | 25.07 ± 0.70 | 27.55 ± 0.36 | 26.24 ± 2.29 |
| Brimful volume | ml | 194.40 ± 0.66 | 196.12 ± 0.26 | 195.11 ± 0.52 | 193.93 ± 0.17 | 197.91 ± 2.72 |
| Total height | m | 179.75 ± 0.02 | 180.04 ± 0.00 | 180.09 ± 0.02 | 180.15±+0.04 | 180.17 ± 0.20 |
| Height under pilver proof | mm | 16.73 ± 0.01 | 16.78 ± 0.01 | 16.77 ± 0.01 | 16.78 ± 0.01 | 16.90 ± 0.09 |
| Bore diameter | mm | 16.86 ± 0.02 | 16.95 ± 0.02 | 16.89 ± 0.01 | 16.89 ± 0.01 | 16.89 ± 0.00 |
| Crest of thread diameter | mm | 21.62 ± 0.01 | 21.64 ± 0.01 | 21.64 ± 0.02 | 21.66 ± 0.01 | 21.69 ± 0.03 |
| Root of thread diameter | m | 19.81 ± 0.02 | 19.84 ± 0.02 | 19.86 ± 0.03 | 19.87 ± 0.02 | 19.87 ± 0.02 |
| Body diameter | mm | 46.46 ± 0.05 | 46.46 ± 0.06 | 46.49 ± 0.07 | 46.45 ± 0.03 | 46.48 ± 0.04 |
| Wall thickness | mm | 0.28 ± 0.16 | 0.27±+0.03 | 0.24 ± 0.04 | 0.25 ± 0.07 | 0.23 ± 0.14 |
| Topload | N | >200 | >200 | >200 | >200 | >200 |

**Fig. 5.** Distortion of the parison at higher processing temperature during extrusion blow molding.

talc in the formulation, which is one of the most effective nucleant for PLA. The thermal transitions observed on the EStr bottle and compound occur at similar temperatures. It is noted, however, that the glass transition temperature measured on the bottle has a value of 1 °C lower than the glass transition temperature of the compound. This decrease is probably attributable to the reduced degree of crystallinity measured on the bottle, as the lack of crystalline structure is certainly associated with a lack of the corresponding rigid amorphous structure in accordance with [26]. Consequently, the glass transition temperature can consistently translate to lower values. In Fig. 1b, it is also interesting to note that, in the third scan, the melting peak of the PLA shifts at lower temperatures and this time the secondary peak on the shoulder of the main peak occurs at higher temperatures. Basically, the concomitant presence of α and α′crystals of PLA is also confirmed in the third scan. The former, as known, are associated with a perfect crystalline structure of PLA, thus presenting a higher melting temperature. The latter are always crystals with a similar structure to the former, but slightly distorted, which is associated with slightly lower melting temperatures [25]. The proportions between the crystals α and α′therefore tends to change between the first and second scans, with the latter becoming predominant. In reality, it can be hypothesized that the α′crystals are the result of crystallization processes that occur more slowly and at lower temperatures, a condition that can be found in the second scan at DSC, where cooling occurs in a controlled manner (10 °C/min). In transformation processes by extrusion blow molding, the cooling is instead forced by the contact of the material with the cold mold wall and takes place in a few seconds, not favoring the formation of the crystalline phase α'.

This result is in partial contrast with what discussed in Ref. [25], where the formation of the crystalline phase α′ is exclusively associated with the value assumed by the crystallization temperature. These authors stated that for cold crystallization temperatures lower than 100 °C only crystalline phase α′ is formed and that for temperatures between 100 and 120 °C both crystalline phase α and α′ are formed, although the latter is favored where the phenomena occur in the low range of the mentioned thermal interval. The results in Fig. 1b, however, show that, in reality, for the EStr bottle the cold crystallization temperature in the third scan (between 100 and 120 °C) is higher than that in the first scan (slightly below 100 °C), although, in the third scan, the peak associated with the crystalline phase α′ is the dominant one. Therefore, the role of crystallization times as well as temperatures in contributing to the formation of the two different crystalline phases is unquestionable. On the other hand [25], studied the formation of crystalline phases of PLA by conducting very long experiments, where the kinetic aspects did not play any role, unlike thermodynamic phenomena, which were the only controlling ones.

The thermograms in Fig. 1c–f can be uniquely discussed. In the first scan, the following primary and secondary transitions are visible respectively: (i) the glass transition temperature of the PLA just before 60 °C; (ii) the exothermic peak of cold crystallization of PLA (87–89 °C depending on the specific formulation examined); (iii) the endothermic melting peak of PBS (~114 °C); (iv) the exothermic peak associated with the transformation (i.e., transition) in the solid phase from the crystalline phase α′ to the phase α (~157–158 °C); (v) the endothermic melting peak of PLA (~174 °C) following the solid phase transition between the crystalline phases α′ to the α phase. The solid phase transition from the α′ crystalline phase to the α phase is present in all cases, since cold crystallization occurs at temperatures clearly below 100 °C in accordance with [25]. This transition to the solid phase is followed by the fusion of the crystalline phase α, thus formed. It is also noted an increase in the glass transition temperature and a corresponding reduction in the cold crystallization temperature by increasing the talc content in the bottle body. This result is in apparent contradiction with what was observed in the compound, where the presence of talc was hypothesized to reduce the glass transition temperature due to the steric effect. The degree of crystallinity of the ES4, ES5, ES6 and ES7 bottles varies, however, between a minimum of 11.7% and a maximum of 19%, higher values than

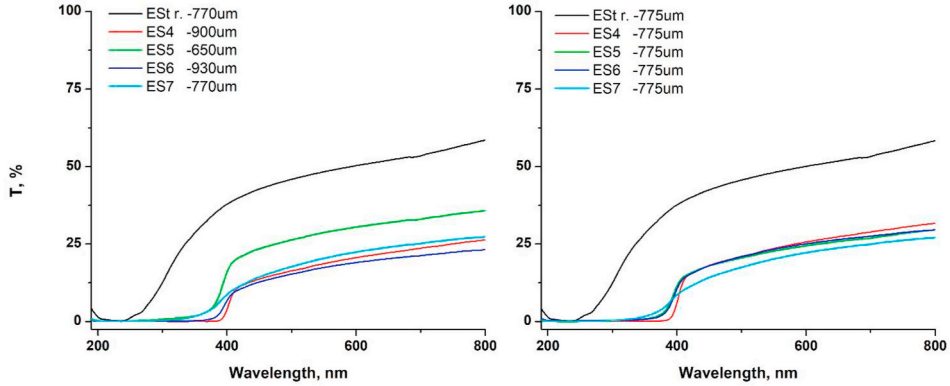


**Fig. 6.** UV-VIS spectra of the EStr, ES4, ES5, ES6 and ES7 bottles: (left) as-is samples; (right) after thickness normalization.

**Table 10**
Thickness of the bottle body. An average nominal thickness of 775 μm was taken to normalize the results.

| Formulation | EStr. | *ES4* | *ES5* | *ES6* | *ES7* |
|---|---|---|---|---|---|
| Thickness | 770 ± 40 | 900 ± 15 | 650 ± 10 | 930 ± 10 | 770 ± 2 |

those found in the corresponding compounds (from 7.5 to 15.6%), but above all very higher than the crystallinity values found for the Estr bottle ($X_c$ 3.2%). In the body of the bottles, the talc content therefore plays a very significant role, as it promotes the formation of a widespread crystalline structure in the PLA, favoring its crystallization, which occurs with greater efficiency and at lower temperatures. Talc, therefore, favors the increase of the glass transition temperature in accordance with [26], as the crystalline structure is associated with a greater presence of a rigid amorphous structure, which determines a corresponding increase in the temperature of glass transition. This effect of talc as a nucleating agent is very clear from the analysis of the second scan (in cooling) for all ES4, ES5, ES6 and ES7 thermograms carried out on the bottle body. In fact, as the talc content increases, the peaks associated with the crystallization of PLA and PBS are increasingly sharper, with more intense phenomena and which start from higher temperatures during the cooling scan. These crystallization peaks are therefore extremely neat in the ES6 and ES7 bottles, to fade into the ES5 bottle and, even more, in the ES4 bottle which have a lower talc content. The third scan (heating) shows very clearly the corresponding heats released by the fusion of PBS and PLA. As the talc content increases, the heat of fusion released increases. In all cases, however, the melting peak of PLA is bimodal, with a small lateral peak attributable to the crystalline phase α′and the main peak, at higher temperatures, attributable instead to the formation of the main crystalline phase α. The presence of the α′phase is not surprising both in relation to the crystallization temperatures observed in the second scan, and in relation to the slowness of the cooling of the material carried out during the second scan in cooling. Finally, in the first and third scans, for the ES4, ES5, ES6 and ES7 formulations, a wide endothermic band around 225 °C, not very deep, can be associated with the heat of fusion of the stereo-complexes between the L and D isomers of the polylactic acid, used in the formulations [20].

Fig. 2 shows an image of the compounds achieved by tween-screw extrusion of the different formulations. These compounds were subsequently used for the manufacturing of the 187.5 ml bottles body. Table 7 summarizes the MFI of the compounds. Increasing the amount of talc in the blends, MFI strongly decreases despite the correction of the rheology of the formulation with higher talc concentration by adding the Luminy L105 (that is, the PLA grade with lower molecular weight and higher MFI). This result agrees only partially with (W. P.-A. Pivsa-Art 22–24 April 2013), where the addition of talc to PLA/PBS (4:1) blends was found to cause a slighter decrease in MFI (only 20% by increasing of 20% the talc concentration).

The compounds were processed by extrusion blow molding process to form the 187.5 ml bottles. The cycle time was ~15 s. The process parameters used during the extrusion blow molding of the bottles were summarized in Table 8. Fig. 3 shows the corresponding parison, whose shape is perfectly cylindrical without any undesired phenomenon of swelling or sagging.

The increase in the percentage of mineral inside the formulation caused a slight increase in the process temperatures, in order to obtain the desired rheological stability of the material [27], according to what is shown in Fig. 3. Fig. 4 shows the result obtained for each formulation. The bottles have a pleasant aesthetic appearance, with a mother-of-pearl color conferred by the PLA present in all formulations and by the micronized talc present, however, only in the formulations based on PLA/PBS in accordance with [17,28]. The weight, the main dimensional characteristics and the resistance to the application of an apical load of 200 N were reported in Table 9. The results are reported in terms of means and relative standard deviations of minimum five measurements. The mass of the bottles increases as the talc concentration in the formulation increases. This can be ascribed to the corresponding increase in the density of the materials. The results are highly repeatable, except for ES7 bottles. ES7 was the most complicated to blow because the low fluidity of the material (MFI 20 g/10 min at 230 °C, 2.16 kg). Increasing processing temperatures for ES7 caused severe sagging and swelling of the parison, not allowing the blowing of the bottle body Fig. 5. The characteristic dimension of the bottles was also very stable for all the compounds investigated. The greatest differences were found in the measurement of the wall thickness of the bottle body. The wall thickness decreases as the talc concentration inside the processed formulation increases. This result is attributable to the greater shrinkage caused by the greater crystallinity of the formulations that contain more talc and crystallize rapidly. The EStr bottle also shows great variation of the wall thickness. EStr compound is very complicated to process, as it is based on a PLA/PBSA blend characterized by a strong difference between their melting peak temperatures. Identifying the correct balance between the contrasting needs of the two materials, which in any case form a binary blend with two immiscible phases [22]. Similarly, ES7 compound is also troublesome to process due to its scarce flow capacity that causes a high variability of wall thicknesses. For these materials, the identification of stable working conditions is very troublesome in accordance with what is reported in Refs. [14,27]. All the bottles passed the 200 N load test, showing satisfactory mechanical response.

Fig. 6 shows the comparison of the spectra obtained for the bottles made with the different formulations under study. The graph on the left shows the compared spectra as obtained, for the various samples with different real thickness (Table 10). In the graph on the right, the same spectra have been mathematically processed through normalization according to the optical absorption for a nominal thickness of 775 μm. Considering the approximation that the back-scattering and diffusion

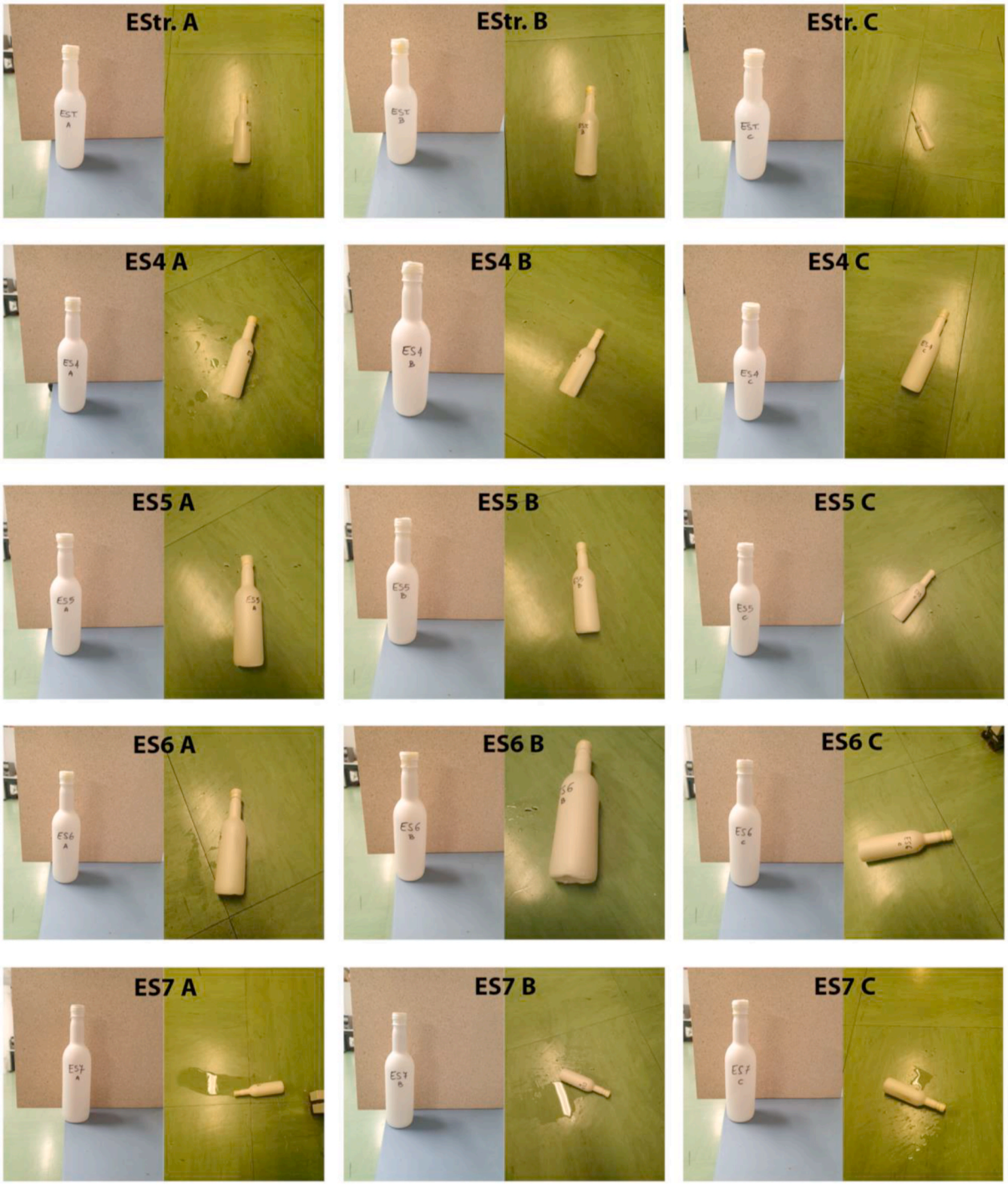


**Fig. 7.** Impact tests of the bottles (vertical drop).

effects of radiation, such as molecular absorption (L-Beer), are directly proportional to the optical path (barrier linked to thickness), and neglecting the compositional variations of the polymeric matrices of the individual formulations, which, in turn, can determine small variations in terms of optical absorption at UV–Vis, the following results are observed for the normalized graphs: (i) the percentage transmittance is maximum for the EStr sample, so-called "transparent", which is proved to be the sample with the least ability to inhibit the transmission of light in the UV and visible spectrum, showing a value that is close to 60% of optical transmission in the red region, but also a reduced barrier in the ultraviolet region beyond the threshold of 250 nm; (ii) the formulations with increasing talc content show a substantial drop in optical transmission, with optical transmission values in the visible region reaching for all the level of about 25%, while showing a total barrier to the transmission of the light radiation for the whole UV region (up to 400 nm); (iii) the last sample of the series, ES7, which has the highest talc content, is characterized by even lower visible transmittance values, which reach 25% at high wavelengths. However, a slight decrease in the UV transmission barrier properties is noted, in particular in the 350–380 nm range, which could be attributed to a certain non-uniformity of the wall thickness.

Fig. 7 and Fig. 8 show the results of the bottle drop tests carried out starting, respectively, from vertical and horizontal position. From the results summarized in Table 11, it can be observed, in general, an

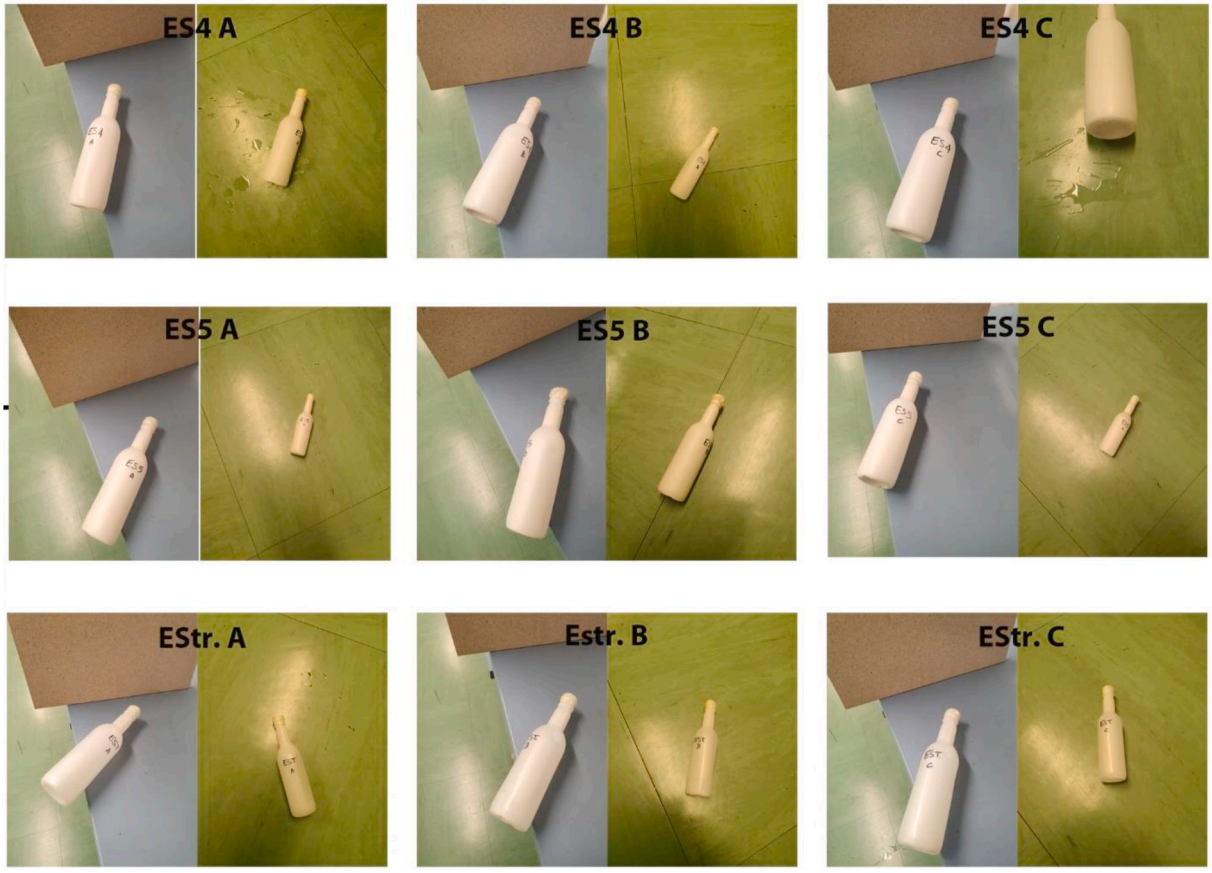


**Fig. 8.** Impact tests of the bottles (horizontal drop).

**Table 11**
Results of the drop tests.

| Tester | EStr. | | | ES4 | | | ES5 | | | ES6 | | | ES7 | | |
|---|---|---|---|---|---|---|---|---|---|---|---|---|---|---|---|
| | *A* | *B* | *C* | *A* | *B* | *C* | *A* | *B* | *C* | *A* | *B* | *C* | *A* | *B* | *C* |
| **Vertical drop** | o | o | o | o | o | o | o | o | o | x | x | x | x | x | x |
| **Horizontal drop** | o | o | o | x | o | x | o | o | o | – | – | – | – | – | – |

increasing fragility of the samples passing from the EStr formulation, the most ductile and impact resistant of the series, up to the more fragile formulations ES6 and ES7. In the order EStr> ES4> ES5> ES6> ES7, that is, as the talc content increases, a tendency to embrittlement of the bottle is observed. The only exception to the trend is shown by the ES5 sample which passed both drop test conditions, similar to the EStr sample. Clearly, this result may also depend on the lack of standardization of the production process, which is still in the prototyping state. This can determine slight differences in the dimensional characteristics of the bottles which can be reflected in behavior in the drop test that is not perfectly consistent with the same formulation.

Fig. 9 shows, in greater detail, the results of the drop tests. The samples with a higher talc content, therefore with a higher degree of crystallinity and considered more fragile, show cracks at key points of the product. In particular, the presence of fractures on the bottom or on the side of the bottle body is noted precisely in correspondence with the rejoining of the flow lines of the extruded material. In this regard, note that the material is extruded in the form of a parison using a torpedo-type mandrel during the blowing process. This type of mandrel requires the separation of the polymeric melt which is subsequently forced to rejoin due to the geometry of the die as well as because of temperature and pressure in it. However, the bioplastic material shows a strong inertness to the rejoining of the flow lines, especially in the case of the brittle formulations characterized by higher talc content. In such cases, the welding of the bioplastic material is only partial, representing such internal welding lines an element of weakness for the structure of the bottle.

Fig. 10 shows the adaptation of the clamping system for measuring gas permeability (oxygen and water vapor) of the bottles which have an oblong geometry, thus requiring a chamber and a dedicated sample holder. Fig. 11 and Fig. 12 show, instead, the typical trends of oxygen and water vapor permeability tests, conducted on the bottle manufactured with the ES7 formulation. In particular, in the left graph, it is possible to see the calibration curve and, in the right graph, the typical trend of the permeability test, respectively, for oxygen (Fig. 11) and for water vapor (Fig. 12). Table 12, on the other hand, summarizes the main results obtained and the relative operating conditions used on all the tested samples, i.e. the ES5, ES6 and ES7 bottles. The EStr and ES4 bottles presenting zero or lower micro-lamellar talc content and the lower degrees of crystallinity were not tested, as they were not considered promising for the purposes of this work.

Since the thicknesses of the side wall of the bottles studied are variable, Table 12 shows the data obtained from the examination of the bottles as they are and, in addition, the OTR and WVTR data suitably


**Fig. 9.** Results of the drop tests.

**Fig. 10.** Experimental set-up for the evaluation of the barrier properties of the bottles.

normalized with respect to the nominal thickness of 775 μm, the same previously used in the analysis of optical transmission tests. This is possible since, with the same volume of the two products under comparison, and therefore of extension of the exchange surface, the only factor that can affect the gas barrier properties, in addition to the intrinsic characteristics of the material, is the bottle thickness that is linked to it in a proportional way. By comparing the OTR and WVTR indices, it is observed that the samples characterized by the highest talc content exhibit the most effective behavior. This result is to be ascribed to the geometric effect of talc which hinders the transmission of gaseous molecules through the bottle wall in accordance with [29] and, at the same time, to the greater degree of crystallinity of the characterized bottles by greater presence of talc. In fact, a high crystallinity content allows to reduce the free volume in the polymer, allowing to reduce its permeability to gases [30]. Similarly, the tasting tests of the wine packaged in ES5, ES6 and ES7 bottles have shown (Fig. 13), even after 4 weeks, an absence of alteration of the flavour of the wine, a constancy of the level of the wine inside the bottle, a color conforms to the original color as well as a constant alcohol content. Therefore, formulation such as ES5 with talc content slightly lower than 20% are already sufficient to ensure adequate protection of the wine over short periods of time, while allowing easy processability in the extrusion blow molding of the bottle and a sufficient resistance to the impact of the same. Wine tests over longer storage time intervals will, however, allow to identify the real shelf life of the product packaged in bioplastic bottles, although most of the rapid deterioration of wine occurs, notoriously, in the first weeks of packaging [31].

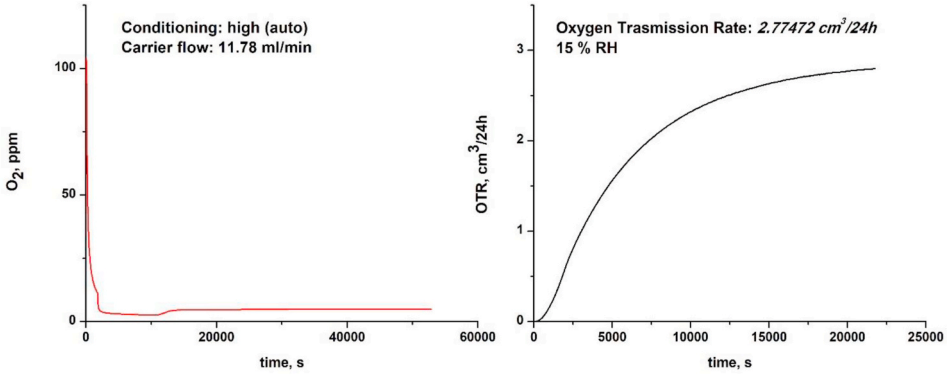


**Fig. 11.** Calibration and typical oxygen permeability test on the ES7 bottle.

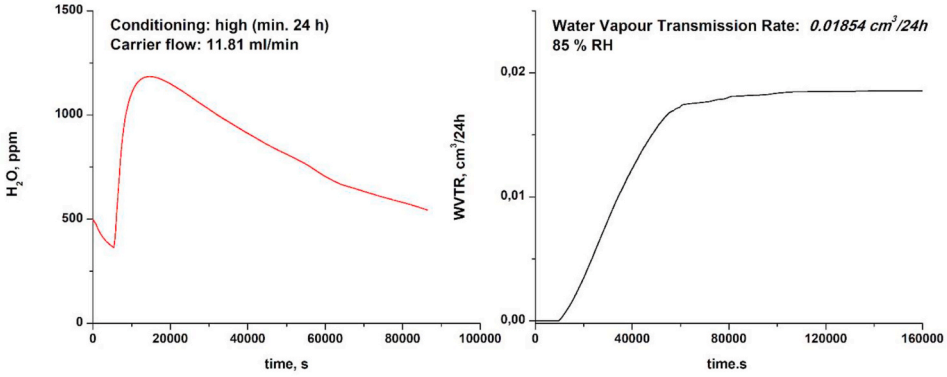


**Fig. 12.** Calibration and typical water vapor permeability test on the ES7 bottle.

**Table 12**
Results of the oxygen and water vapor permeability test.

| *Permeability* | *$O_2$ Transmission* OTR 23 °C - RH 15% ($cm^3$/ 24 h) | | *$H_2O$ Transmission* WVTR 23 °C - RH 85% ($cm^3$/ 24 h) |
|---|---|---|---|
| ***ES5*** | **OTR 100%** | 0.70885 | 0.03080 |
| | **OTR 21%** | 0.14886 | |
| ***ES5 NORM* 775 µm ($s_m = 700 \pm 300$ µm)** | **OTR 100%** | 0.64025 | 0.02782 |
| | **OTR 21%** | 0.13445 | |
| ***ES6*** | **OTR 100%** | 0.71956 | – |
| | **OTR 21%** | 0.15110 | |
| ***ES6 NORM* 775 µm ($s_m = 800 \pm 350$ µm)** | **OTR 100%** | 0.74277 | – |
| | **OTR 21%** | 0.15598 | |
| ***ES7*** | **OTR 100%** | 0.76859 | 0.01854 |
| | **OTR 21%** | 0.16140 | |
| ***ES7 NORM* 775 µm ($s_m = 530 \pm 150$ µm)** | **OTR 100%** | 0.85948 | 0.01268 |
| | **OTR 21%** | 0.18049 | |

## 4. Conclusions

This work studies the applicability of different bioplastic formulations in the manufacturing process of low environmental footprint bottles for the packaging of alcoholic beverages and, in particular, wine. Both PLA/PBSA and PLA/PBS binary blends were studied, the latter characterized by the presence of micronized lamellar talc. Specifically, the reactive extrusion processes with a co-rotating twin-screw extruder of the various formulations were studied, as well as the related extrusion blow molding processes for the manufacture of the bottles. The bottles were also evaluated for their thermo-mechanical and physical behavior. Based on the experimental results, the following conclusions can be drawn:

- The thermal analysis showed that bottles involving formulations with a higher talc content have a higher crystallization rate, but a lower glass transition temperature when the talc content is increased. However, formulation ES7 that shows the lowest Tg is modified by the addition of acrylate-based impact modifiers that are known to be able to slightly reduce the Tg;
- Thermal analysis of the bottles allows to discern between the different types of PLA crystals that can be formed during the extrusion compounding and extrusion blow molding process according to the crystallization kinetic of the materials;
- The extrusion blow molding process of the bottles must account for the rheological behavior of the different formulations: setting the correct process temperatures both in the extrusion phase and in the die-head made it possible to control the swelling and sagging of the parisons, ensuring good processability for most of the bioplastics investigated;
- Increasing the talc content in the formulations allows to achieve the best results in terms of reduction of light and gas transmission through the bottle wall; in contrast, an increase in talc content cause an embrittlement of the bottle, which is less prone to withstand the drop test;


**Fig. 13.** Wine testing after 1, 14, 21 and 28 days.

- ES5 compounds that involve talc concentration slightly lower than 20% are sufficient to ensure wine protection on short time range, allowing, at the same time, an easy processability of the material in extrusion blow molding of the bottle as well as a sufficient impact resistance of the bottle itself during the drop tests.
- The cost of the formulation amounts to approximately 3.30 Eur/kg at raw material prices in April 2021. However, prices are highly fluctuating. The price per bottle is aligned with the price of the corresponding glass bottle (about 13–14 cents/piece) in the case of modest volumes (~five million pieces) and considering that no investments are necessary for the latter. For higher volumes, bioplastic becomes more competitive than glass in relation to the economies achievable on the mold.

Ultimately, bioplastic materials have made it possible to obtain, following an adequate development of the production process, bottles of good quality for wine packaging with a continuous and reproducible production cycle. Although further evaluations on the functional properties of the bottles will be necessary (in particular, gas permeability, stability in contact with alcohol, wine shelf time), they can be certainly proposed as a valid ecological alternative to the current plastic bottles from source fossil or other, more pollutant, solutions used for the packaging of alcoholic beverages, such as laminates and bag-in-box.

## Credit author statement

Conceptualization:*All authors*. **Methodology:** *All authors*. **Software:** *Not available*. **Validation:** *Pizzi, Aversa*. **Formal analysis:** *Not available*. **Investigation:** *All authors*. **Resources:** *Barletta, Prati*. **Data Curation:** *All authors*. **Writing - Original Draft:** *All authors*. **Writing - Review & Editing:** *All authors*.**Visualization:** *All authors*. **Supervision:** *Barletta*. **Project administration:** *Barletta*. Funding **acquisition:** *Barletta*.

## Conflicts of interest

The authors acknowledge there is no conflict of interest about the content of this manuscript.

## Declaration of competing interest

The authors declare that they have no known competing financial interests or personal relationships that could have appeared to influence the work reported in this paper.

## Acknowledgements

The authors wish to warmly thank Claudia Berardi, researcher of Serioplast Spa, for the contribution offered in the molding of the bottles and in the relative characterization tests.

## References

[1] F. Licciardello, Packaging, blessing in disguise. Review on its diverse contribution to food sustainability, Trends Food Sci. Technol. 65 (2017) 32–39.
[2] C.Y. Barlow, D.C. Morgan, Polymer film packaging for food: an environmental assessment, Resour. Conserv. Recycl. 78 (2013) 74–80.
[3] B. Yun, P. Bisquert, P. Buche, M. Croitoru, V. Guilard, R. Thomopoulos, Choice of enviroment-friendly food packages through argumentation systems and preferences, Ecological Informations 48 (2018) 24–36.
[4] F. Wilkstrom, H. Williams, K. Verghese, S. Clune, The influence of packaging attributes on consumer behaviour in food-packaging life cycle assessment studies - a neglected topic, J. Clean. Prod. 73 (2014) 100–108.
[5] C. Ferrara, e G. De Feo, Life Cycle Assessment application to the wine sector: a critical review, Sustainability 10 (2) (2018) 395–410.
[6] R. Accorsi, L. Versari, e R. Manzini, Glass vs. plastic: life Cycle Assessment of extra-virgin olive oil bottles across global supply chains, Sustainability 7 (3) (2015) 2818–2840.
[7] C. Ferrara, V. Zigarelli, e G. De Feo, Attitudes of a sample of consumers towards more sustainable wine packaging alternatives, J. Clean. Prod. 271 (2020) 122581.
[8] C. Ferrara, e G. De Feo, Comparative life cycle assessment of alternative systems for wine packaging in Italy, J. Clean. Prod. 259 (2020) 120888.
[9] Simone Nessi, Lucia Rigamonti, e Mario Grosso, LCA of waste prevention activities: a case study for drinking water in Italy, J. Environ. Manag. 108 (2012) 73–83.
[10] C. Castellon, e E. Clevis, Empaque bag in box en industria agrícola y su impacto en el medio ambiente, Thesis, Universitat Politècnica de Catalunya, Barcelona, Spain, 2019.
[11] M. Bertolini, E. Bottani, G. Vignali, e A. Volpi, Comparative life cycle assessment of packaging systems for extended shelf life milk, Packag. Technol. Sci. 29 (10) (2016) 525–546.
[12] M. Barletta, C. Aversa, M. Puopolo, S. Vesco, Extrusion blow molding of environmentally friendly bottles in biodegradable polyesters blends, Polym. Test. 77 (2019) 105855.

[13] M. Karamanlioglu, R. Preziosi, e G.D. Robson, Abiotic and biotic environmental degradation of the bioplastic polymer poly(lactic acid): a review, Polym. Degrad. Stabil. 137 (2017) 122–130.
[14] W. Rodriguez-Castellanos, F. Martinez-Bustos, D. Rodrigue, e M. Trujillo-Barragan, Extrusion blow molding of a starch–gelatin polymer matrix, Eur. Polym. J. 73 (2015) 335–343.
[15] R. Ghidossi, et al., The influence of packaging on wine conservation, Food Contr. 23 (2) (2012) 302–311.
[16] J.J. Kolstad, Crystallization kinetics of poly(l-lactide-co-mesolactide), J. Appl. Polym. Sci. 62 (1996) 1079–1091.
[17] C. Aversa, M. Barletta, E. Pizzi, M. Puopolo, e S. Vesco, Wear resistance of injection moulded PLA-talc engineered bio-composites: effect of material design, thermal history and shear stresses during melt processing, Wear 390–391 (2017) 184–197.
[18] L.T. Lim, R. Auras, e M. Rubino, Processing technologies for poly(lactic acid), Prog. Polym. Sci. 33 (2008) 820–852.
[19] H. Tsuji, Poly(lactide) stereocomplexes: formation, structure, properties, degradation, and applications, Macromol. Biosci. 5 (2005) 569–597.
[20] H. Tsuji, e I. Fukui, Enhanced thermal stability of poly (lactide)s in the melt by enantiomeric polymer blending, Polymer 24 (2003) 2891–2896.
[21] W. Pivsa-Art, S. Pivsa-Art, Effect of talc on mechanical characteristics and fracture toughnessof Poly(lactic acid)/Poly(butylene succinate) blend, J. Polym. Environ. 27 (2019) 1821–1827.
[22] D. Lascano, L. Quiles-Carrilo, R. Balart, T. Boronat, N. Montanes, Toughened Poly (Lactic Acid)—PLA formulations by binary blends with Poly(Butylene Auccinate-co-Adipate) - PBSA and their shape memory behaviour, Materials 12 (2019) 622–635.
[23] H. Tsuji, H. Takai, N. Fukuda, H. Takikawa, Non-Isothermal crystallization behavior of Poly(L-lactic acid) in the presence of various additives, Macromol. Mater. Eng. 291 (4) (2006) 325–335.
[24] F. Yu, T. Liu, X. Zhao, X. Yu, A. Lu, J. Wang, Effects of talc on the mechanical and thermal properties of polylactide, J. Appl. Polym. Sci. 125 (S2) (2012) E99–E109.
[25] T. Tabi, S. Hajba, e J.G. Kovacs, Effect of crystalline forms (α′ and α) of poly(lactic acid) on its mechanical, thermo-mechanical, heat deflection temperature and creep properties, Eur. Polym. J. 82 (2016) 232–243.
[26] K. Zhang, V. Nagarajan, M. Misra, A.K. e Mohanty, Supertoughened renewable PLA reactive multiphase blends system: phase morphology and performance, Applied Materials & Interfaces 6 (15) (2014) 12436–12448.
[27] A. Attar, N. Bhuiyan, V. Thomson, Manufacturing in blow molding: time reduction and part quality improvement, J. Mater. Process. Technol. 204 (2008) 284–289.
[28] C. Aversa, M. Barletta, A. Gisario, E. Pizzi, M. Puopolo, e S. Vesco, Improvements in mechanical strength and thermal stability of injection and compression molded components based on Poly Lactic Acids, Adv. Polym. Technol. 37 (6) (2018) 2158–2170.
[29] A. Buzarovska, G. Bogoeva-Gaceva, e R. Faigar, Effect of the talc filler on structural, water vapor barrier and mechanical properties of poly(lactic acid) composites, J. Polym. Eng. 36 (2) (2015) 181–188.
[30] V.P. Shantarovich, I.B. Kevdina, Y.P. Yampolskii, e A.Y. Alentiev, Positron annihilation lifetime ltudy of high and low free volume glassy polymers: Effects of free volume sizes on the permeability and permselectivity, Macromolecules 33 (20) (2000) 7453–7466.
[31] A.W. Linsenmeier, D. Rauhut, e W.R. Sponholz, Ageing and flavour deterioration in wine, Managing Wine Quality 16 (2010) 459–493.